



## Crack tip fields in elastic-plastic and mixed mode I+II+III conditions, finite elements simulations and modeling

F. Fremy, S. Pommier

LMT (ENS Cachan / CNRS / Université Paris Saclay)

Flavien.Fremy@ens-cachan.fr, Sylvie.Pommier@ens-cachan.fr

E. Galenne

EDF R&D

Erwan.Galenne@edf.fr

S. Courtin

Areva NP

Stephan.Courtin@areva.com

**ABSTRACT.** This paper is devoted to the analysis of the load path effect on I+II+III mixed mode fatigue crack propagation in a 316L stainless steel. Experiments were conducted in mode I+II and in mode I+II+III. The same maximum, minimum and mean values of the stress intensity factors were used for each loading path in the experiments. The main result of this set of experiments is that very different crack growth rates and crack paths are observed for load paths that are however considered as equivalent in most fatigue criteria. The experiments conducted in mode I+II and in mode I+II+III, also allowed to show that the addition of mode III loading steps to a mode I+II loading sequence is increasing the fatigue crack growth rate, even when the crack path is not significantly modified.

**KEYWORDS.** Fatigue crack growth; Mixed mode; Mode I; Mode II; Mode III.

### INTRODUCTION

Most cyclically loaded machines are subjected to multi-axial loadings. For example, power shafts are usually subjected to a combination of torsion and bending due to the transmission of the torque, the self-weight of the shaft and its rotation speed.

For components loaded in proportional multi-axial conditions, the fracture mechanics concepts are normally used to determine the crack path for which the crack is loaded in mode I [1-7]. Then, the growth rate is usually predicted using the Paris' law determined in mode I conditions. When non-proportional multi-axial loading conditions are encountered, various approaches have been derived from the Paris' law, to predict the growth rate in mixed mode conditions [1-3]. Most of them are based on an equivalent stress intensity factor (Eq. 1), whose expression varies according to the authors, but is usually function of the stress intensity factor ranges (Eq. 2).

$$\frac{da}{dN} = CK_{eq}^m \quad (1)$$

$$\Delta K_{eq} = \left( \Delta K_I^n + \beta \Delta K_{II}^n + \gamma \Delta K_{III}^n \right)^{1/n} \quad (2)$$

Corrections are required to account for the closure effect, or for the in-phase or out-of-phase nature of the fatigue cycles. As a matter of fact, most papers devoted to fatigue crack growth under out-of-phase or sequential mixed mode loading conditions indicate a detrimental effect of the mode-mixity variation during the fatigue cycle and do underline the role of crack tip plasticity [1-7].

A set of experiments was therefore conducted in order to characterize specifically the importance of the load path effect on mixed mode fatigue crack growth, all the other effects being as far as possible kept the same. In these experiments, the stress intensity factor ranges and mean values are the same for each mode and each load path. A static mode I load is always applied so as to limit the effect of crack closure. The tests were conducted with different load paths, yet both "in phase" or both "out of phase", in the sense that the extremes values of the stress intensity factors in each mode are attained simultaneously or not.

## EXPERIMENTS

### *Material & Experimental setup*

The tested material is an AISI 316 L austenitic stainless steel. This material is employed in power plants to produce various components such as pumps, mixing tees and taps because of its excellent resistance to corrosion, its good formability and ductility. The elastic-plastic behavior of this material has been extensively studied in uniaxial and multiaxial conditions [8].

The experiments were conducted on the multiaxial servo-hydraulic testing machine ASTREE, available at LMT-Cachan. Six actuators are used simultaneously to perform the tests (Fig. 1). Three pairs of actuators are used to load the specimen along three orthogonal axes and to keep fixed the intersection of the three loading axes fixed. Each horizontal loading axis is load controlled.

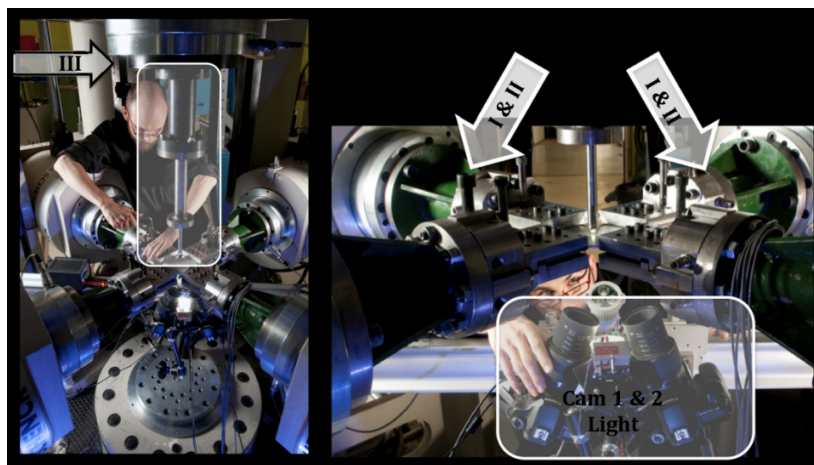


Figure 1: Six actuators servo-hydraulics testing machine ASTREE, experimental set-up.

A cruciform specimen was used for the experiments (Fig. 2). A centered 30 mm long slit is machined in the specimen (Fig. 2), the slit plane being inclined at 45° with the loading axes of the specimen.

Linear elastic finite element analyses were conducted in order to determine the relations between the loads FX, FY and FZ applied along the three axes of the specimen (Fig. 2) and the stress intensity factors KI, KII and KIII at mid-thickness for a coplanar crack propagating from the slit. A mode I stress intensity factor is obtained by applying the same load along the two in-plane axes of the specimen (FX=FY). A mode II stress intensity factor is obtained by applying FX=-FY. A mode III stress intensity factor is obtained by applying an out-of-plane load FZ.

The mode I+II+III loading cycles used in the experiments do always include a positive mean value of KI, for three main reasons. First of all, a positive mean value of KI allows limiting the crack closure effects. Second, the mean value of KI was determined so that the in-plane loads FX and FY will always remain positive during cycling so as to avoid any buckling of the specimen. Third, when an out-of-plane load FZ is applied onto the specimen, it induces a bending of the

specimen and hence it induces a mode I stress intensity factor variation along the crack front. This variation was determined using finite element analyses. It was checked that, for the mixed mode I+II+III fatigue cycles used in these experiments, the mode I stress intensity factor induced by the application of the out-of-plane load  $F_Z$  could be neglected with respect to the mode I stress intensity factor induced by the application of the in-plane loads  $F_X=F_Y$ .

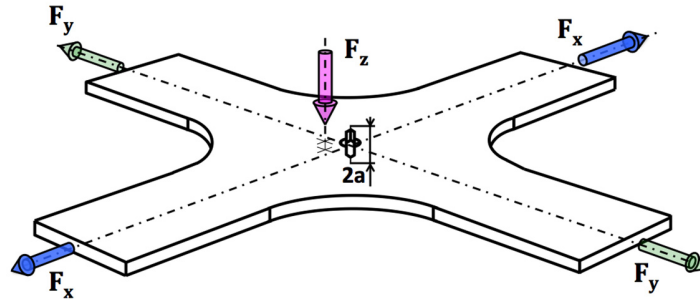


Figure 2: Schematics of the specimen and of the boundary conditions.

### Loading cases

Each specimen was pre-cracked in mode I at 10 to 20 Hz and at  $R=0.33$  ( $\Delta F_X=\Delta F_Y=33.1$  kN,  $F_Z=0$  kN) up to a crack length  $2a=34$  mm. For this crack length, the stress intensity factors used to pre-crack the specimen corresponds to  $K_{Imin}=5$  MPa $\sqrt{m}$  and  $K_{Imax}=15$  MPa $\sqrt{m}$ .

Each load path considered in this set of experiments is defined by means of evolutions of the stress intensity factors  $K_I(t)$ ,  $K_{II}(t)$  and  $K_{III}(t)$ . For a crack length  $2a=34$  mm, the load sequences  $F_X(t)$ ,  $F_Y(t)$  and  $F_Z(t)$  that corresponds to the desired evolutions of the stress intensity factors  $K_I(t)$ ,  $K_{II}(t)$  and  $K_{III}(t)$ , are determined using FE simulations.

The load sequences  $F_X(t)$ ,  $F_Y(t)$  and  $F_Z(t)$  determined for  $2a=34$  mm are then applied to grow the crack by fatigue up to a length of about  $2a=38$  mm. In the following, when values of the stress intensity factors are given, they correspond to the start of the test when  $2a=34$ mm.

Four mixed mode I+II loadings cases have been studied (Fig. 3). Each of them is centered around the same mean value for each mode  $K_I = 10$  MPa $\sqrt{m}$  and  $K_{II} = 0$ , and has the same stress intensity factor amplitude for each mode  $\Delta K_I = \Delta K_{II} = 10$  MPa $\sqrt{m}$ . These four cases are all equivalent with respect to the criteria based on an equivalent stress intensity factor (Eq. 2) determined in linear elastic conditions.

The load paths were constructed as follows:

- first, the peak values of  $K_I$  and  $K_{II}$  are attained simultaneously for the “proportional” (Fig. 3C), the “square” (Fig. 3A) and the “windmill” (Fig. 3D) load paths,
- second, the cumulative “lengths” of the “square” (Fig. 3A) and the “cross” (Fig. 3B) load paths are the same, and is one half of that of the “windmill” (Fig. 3D) load path,
- third, there is one cycle with an amplitude  $\Delta K_I = \Delta K_{II} = 10$  MPa $\sqrt{m}$  in each load path for the “proportional” (Fig. 3C), the “square” (Fig. 3A) and the “cross” (Fig. 3B) load paths. The case of the “windmill” (Fig. 3D) load path is somehow different, since we may either count, per load path, two cycles, with an amplitude  $\Delta K_I = \Delta K_{II} = 10$  MPa $\sqrt{m}$ , or, the sum of one cycle with an amplitude  $\Delta K_I = \Delta K_{II} = 10$  MPa $\sqrt{m}^{1/2}$ . and two smaller cycles with an amplitude  $\Delta K_I = \Delta K_{II} = 5$  MPa $\sqrt{m}$ .

As in mixed mode I+II conditions, the loading cases studied in mixed mode I+II+III conditions (Fig. 4) are centered around the same mean value for each mode  $K_I=10$  MPa $\sqrt{m}$ ,  $K_{II}=0$  and  $K_{III}=5$  MPa $\sqrt{m}$ , and have the same stress intensity factor amplitude for each mode  $\Delta K_I = \Delta K_{II} = \Delta K_{III} = 10$  MPa $\sqrt{m}$ . They are also equivalent with respect to the criteria in Eqs. 2.

In addition,

- the peak values of  $K_I$ ,  $K_{II}$  and  $K_{III}$  are attained simultaneously for the “proportional” (Fig. 4B) and the “cube” (Fig. 4A) load paths,
- the cumulative “lengths” of the “cube” (Fig. 4A) and the “star” (Fig. 4C) load paths are the same,

- the contribution of mode III to mixed mode fatigue crack growth can be determined by comparing pairs of load cases, namely the two “proportional” load paths (Fig. 3C and Fig. 4B), the “square” and the “cube” load paths (Fig. 3A and Fig. 4A) and finally the “cross” and the “star” load paths (Fig. 3B and Fig. 4C).

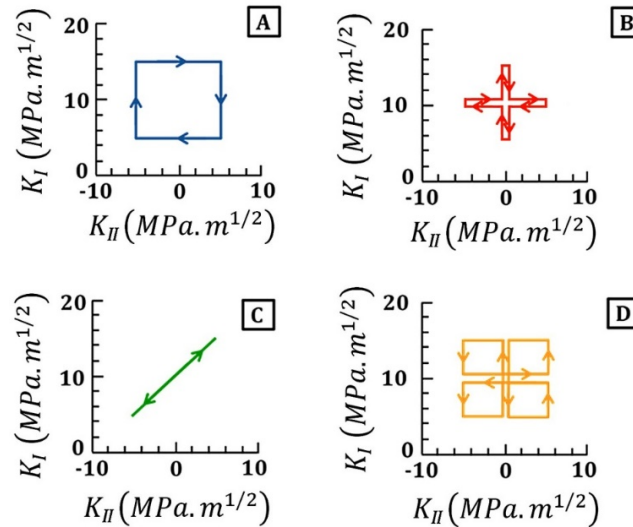


Figure 3: Loading cases applied in mixed mode I+II conditions. A – « Square » load path, B – « Cross » load path C – « Proportional » load path, D – « Windmill » load path.

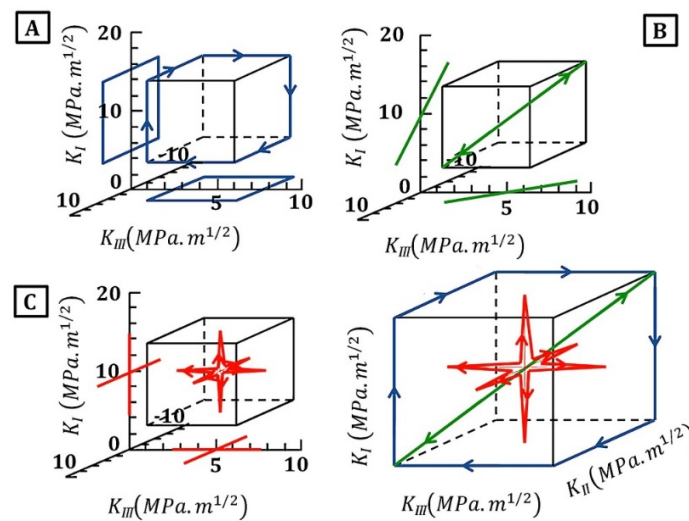


Figure 4: Loading cases applied in mixed mode I+II+III conditions. A – « Cube » load path, B – « Proportional » load path, C – « Star » load path.

## RESULTS

The results of the fatigue crack growth experiments conducted in mixed mode I+II conditions indicate that there is a significant load path effect in mixed mode fatigue crack growth (Fig 5a).

First of all, the crack path is significantly different according to the load path selected. These observations show a significant tilt of the crack path (40°) for the “proportional” load path, after 1 mm of coplanar crack growth in mixed mode conditions. On the contrary, the tilt of the crack path is found to be moderate for the “square” load path (10°) and very small for the two other cases.



Second, in all mixed mode I+II experiments, below 1 mm of crack propagation, the crack path remained coplanar even for the “proportional” load path. The crack growth rate variations from one test to another can thus be attributed to a load path effect only. The number of cycles required to get a crack extent of 0.65 mm, for instance can typically varies by a factor 3, according to the load path applied in the experiment, though the extreme values and the mean values of the stress intensity factors are kept the same in each experiment.

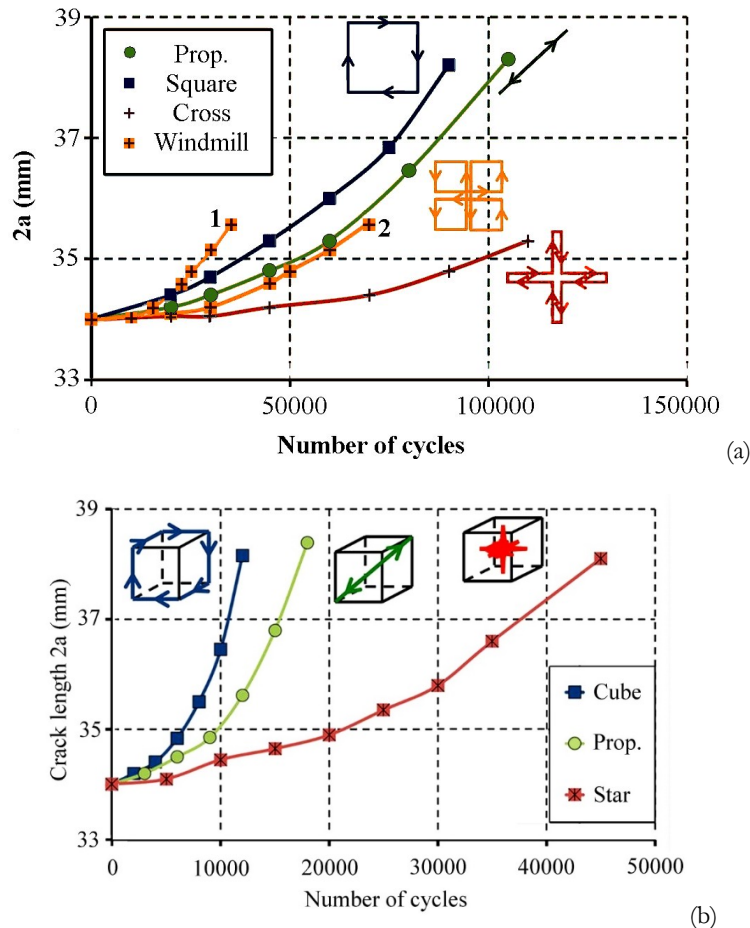


Figure 5: (a) Evolutions of the crack lengths with the number of cycles applied for each load case in mixed mode I+II conditions. Two curves are plotted for the « windmill » load path, the curve 1, was plotted considering 1 cycle per load path, and the curve 2 considering 2 cycles per load path. (b) Evolutions of the crack lengths with the number of cycles applied for each load case in mixed mode I+II+III conditions.

The results of the fatigue crack growth experiments conducted in mixed mode I+II+III conditions are plotted in Fig. 5b. As in mixed mode I+II, a very significant load path effect is observed. However, the load path effect is smaller when the extreme values of the stress intensity factors are attained simultaneously for each mode (“cube” and “proportional” load paths). The largest difference is observed between the “cube” and the “star” load paths.

As in mixed mode I+II, below 0.5 mm the crack path remains coplanar and the variations of the growth rate from one test to the other can solely be attributed to the load path effect. The number of cycles required to grow the crack by  $\Delta a=0.5$  mm in each mode I+II+III test are gathered in Tab. 1. According to the loading path the crack growth rate is found to vary by more than a factor 2. In addition, in mixed mode I+II+III, the crack path is also significantly varying with the loading case. The effects are more pronounced in mixed mode I+II+III than in mixed mode I+II. The overall inclination of the crack path was roughly characterized at the end of the test, by two angles, the tilt angle ( $\alpha$ ) and the twist angle ( $\beta$ ).



Load path	Number of cycles $\Delta N_i$ to get $\Delta a=0.5$ mm	$\Delta N_i/\Delta N_C$	$\Delta K_{eq} = \left( C \frac{\Delta N}{\Delta a} \right)^{\frac{1}{m}}$
Cube	$\Delta N_A=4678$	0.43	30.82
Proportional	$\Delta N_B=6216$	0.57	28.08
Star	$\Delta N_C=10920$	1.00	23.34

Table 1: Number of cycles required to grow the crack by fatigue by  $\Delta a=0.5$  mm in each experiment, equivalent stress intensity factor  $\Delta K_{eq}$  (MPa $\sqrt{m}$ ) required to get a growth rate  $\Delta a / \Delta N_i$  (m / cycle) assuming Eq. 1, with  $m=3$  and  $C=3.08 \cdot 10^{-12}$ .

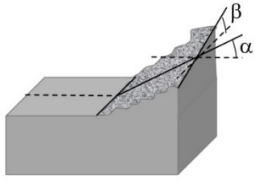
	Load path	“Prop.”	“Cube”	“Star”
	Tilt angle $\alpha$	-10°	none	40°
Twist angle $\beta$	50°	15°	10°	

Table 2: Twist angle ( $\beta$ ) through the thickness of the specimen (5 mm) and tilt angle ( $\alpha$ ) after the crack has propagated in mixed mode by  $\Delta a=2$ mm. Effect of the load path on the crack path, after the crack has propagated in mixed mode I+II+III from  $2a=34$ mm up to  $2a=38$ mm.

The “proportional” loading path has promoted the most severe change in the crack path, since the crack plane has twisted by an angle of about 50°. On the contrary, the fatigue crack growth remains more or less coplanar under the “cube” load path.

Most surprisingly, the “star” load path is producing a significant tilt and a small twist, while no bifurcation was observed in mode I+II under the “cross” load path. Adding mode III loading steps (“star”) to a mixed mode I+II loading cycle (“cross”) did not promote the twisting of the crack path, but induced a tilt.

## CONCLUSIONS

Experiments were conducted in mode I+II and in mode I+II+III non-proportional loading conditions in order to characterize the load path effect in fatigue crack propagation in a 316L stainless steel and the contribution to fatigue crack growth of mode III loadings.

Since the same maximum, minimum and mean values of the stress intensity factors were applied in each experiments, the load paths are all considered as “equivalent” with respect to most of the fatigue crack growth criteria, in particular with those based on  $\Delta K_{eq} = \left( \Delta K_I^n + \beta \Delta K_{II}^n + \gamma \Delta K_{III}^n \right)^{\frac{1}{n}}$ .

The main result of this set of experiments is that very different crack growth rates are observed even though the extreme values and the mean values of the stress intensity factors are the same in each test. A variation by up to a factor three of the crack growth rate according to the loading path was observed in these experiments, even when the crack path remained coplanar.

In addition, it was shown that the crack path is also significantly dependent of the load path. For instance, the crack path remains coplanar for the “square” load path while a tilt is observed for the “proportional” load path in mixed mode I+II. In these two cases, the extreme values of the mode I and mode II stress intensity factors are attained simultaneously.

## REFERENCES

- [1] Qian, J., Fatemi, A., Mixed mode fatigue crack growth: A literature survey. *Engineering Fracture Mechanics*, 55(6) (1996) 969-990.



- [2] Hourlier, F., Pineau, A., Propagation of fatigue cracks under polymodal fatigue, *Fatigue of Engineering Materials and Structures*, 5 (4) (1982) 287-302.
- [3] Bold, P. E., M. W. Brown, A Review of Fatigue Crack-Growth in Steels under Mixed Mode-I and Mode-II Loading, *Fatigue & Fracture of Engineering Materials & Structures*, 15(10) (1992) 965-977.
- [4] Plank, R., Kuhn, G., Fatigue crack propagation under non-proportional mixed mode loading. *Engineering Fracture Mechanics*, 62(2-3) (1999) 203-229.
- [5] Brown, M. W. B., S. L. Wong, Fatigue crack growth rates under sequential mixed-mode I and II loading cycles. *Fatigue & Fracture of Engineering Materials & Structures*, 23(8) (2000) 667-674.
- [6] Doquet, V., Abbadi, M., Influence of the loading path on fatigue crack growth under mixed-mode loading. *International Journal of Fracture*, 159(2) (2009) 219-232.
- [7] Doquet, V., Pommier, S., Fatigue crack growth under non-proportional mixed-mode loading in ferritic-pearlitic steel. *Fatigue & Fracture of Engineering Materials & Structures*, 27(11) (2004) 1051-1060.
- [8] Benallal, A., Legallo, P., An Experimental Investigation of Cyclic Hardening of 316-Stainless Steel and of 2024-Aluminum Alloy under Multiaxial Loadings. *Nuclear Engineering and Design*, 114(3) (1989) 345-353.